JOC Article

Rearrangement of the Cyclohexadiene Derivatives of C_{60} to Bis(fulleroid) and Bis(methano)fullerene: Structure, Stability, and Mechanism

Cherumuttathu H. Suresh,[†] Periya S. Vijayalakshmi,[‡] Sho-ichi Iwamatsu,*[,‡] Shizuaki Murata,[‡,⊥] and Nobuaki Koga[§]

Nagoya University Venture Business Laboratory, Graduate School of Environmental Studies, and Graduate School of Human Informatics, Nagoya University, Nagoya 464-8601, Japan, and CREST, Japan Science and Technology Corporation (JST), Japan

iwmt@urban.env.nagoya-u.ac.jp

Received January 5, 2003

The cyclohexadiene derivative of C_{60} rearranges photochemically to bis(fulleroid) (two [6,5] open structure) and bis(methano)fullerene (two [6,6] closed structure). During this process, a [6,5] open/[6,6] closed intermediate is observed. The isolated intermediate undergoes photochemical rearrangement to bis(fulleroid) and bis(methano)fullerene. On the other side, it undergoes retrorearrangement to the starting material in the dark. The structure and energetics of these C_{60} derivatives have been studied at the AM1, PM3, RHF, and B3LYP levels of theory. It is found that bis(fulleroid) bearing four *tert*-butoxycarbonyl substituents is 5.8 kcal/mol (B3LYP) more stable than the corresponding bis(methano)fullerene. The isolated intermediate having the [6,5] open/[6,6] closed structure is 6.7 kcal/mol more favorable than the previously proposed two [6,5] closed intermediate, and the formation of this compound is well explained by the di-π-methane rearrangement. ^{13}C NMR calculation at the B3LYP level reproduced the experimental chemical shifts with very good accuracy for each molecular system. Theoretical studies mainly at the unrestricted B3LYP level on singlet and triplet state potential energy surfaces on fullerene derivatives support the di-π-methane rearrangement mechanism. The previously proposed symmetrical [4+4]/[2+2+2] and the novel proposed unsymmetrical di-π-methane pathways may coexist during the reaction.

Introduction

Fulleroid, a homologue of C_{60} with a [6,5] open structure, has received much attention since the early discovery by Wudl et al., because it is the only derivative that retains the entire 60π-electron configuration of C_{60}.[1−4] It isomerizes to the methanofullerene ([6,6] closed structure) under a variety of reaction conditions with the one exception of the unsubstituted $C_{61}H_2$ (this can be done by light/thermal, electrochemically, or under acidic conditions) (Scheme 1).[2,3] Generally, fulleroid is a kinetically controlled product, whereas methanofullerene is a thermodynamic product. It is believed that the isomerization proceeds via the [6,5] closed isomer whose cyclopropane ring is produced on the five-membered ring.[2,3] Recently, a detailed kinetic study of the fulleroid−methanofullerene rearrangement reaction was reported by Shevlin et al., and it revealed that the reaction proceeded thermally and photochemically according to the first- and zeroth-order kinetics law, respectively.[3d]

A novel fulleroid derivative bis(fulleroid) (**4a**), containing two [6,5] open structures connected by an ethylene linker, was first produced by Rubin et al. using photochemical rearrangement of the cyclohexadiene derivative of C_{60}.[5] The mechanism of this reaction was explained as follows: in the first step the photochemically allowed [4+4] reaction yielded two [6,5] closed cyclopropane rings

[†] Nagoya University Venture Business Laboratory.
[‡] Graduate School of Environmental Studies, Nagoya University.
[§] Graduate School of Human Informatics, Nagoya University.
[⊥] CREST, Japan Science and Technology Corporation (JST).

(1) For reviews: (a) Hirsch, A. *The Chemistry of Fullerenes*; Thieme Verlag: Stuttgart, Germany, 1994, Chapter 4. (b) Meier, M. S. *The Chemistry of Fullerenes*; Taylor, R., Ed.; World Scientific Publishing: Singapore, 1995; Chapter 9, p 10. (c) *Fullerenes: Chemistry, Physics, and Technology*; Kadish, K. M., Ruoff, R. S., Eds.; John Wiley & Sons: New York, 2000; Chapter 3.

(2) (a) Suzuki, T.; Li, Q.; Khemani, K. C.; Wudl, F.; Almarsson, Ö. *Science* **1991**, *254*, 1186. (b) Wudl, F. *Acc. Chem. Res.* **1992**, *25*, 157. (c) Smith, A. B., III; Strongin, R. M.; Brard, L.; Furst, G. T.; Romanow, W. J.; Owens, K. G.; King, R. C. *J. Am. Chem. Soc.* **1993**, *115*, 5829. (d) Diederich, F.; Isaacs, L.; Philp, D. *J. Chem. Soc., Perkin Trans. 2* **1994**, 391. (e) Diederich, F.; Isaacs, L.; Philp, D. *Chem. Soc. Rev.* **1994**, 244 and references therein.

(3) (a) Eiermann, M.; Wudl, F.; Prato, M.; Maggini, M. *J. Am. Chem. Soc.* **1994**, *116*, 8364. (b) Janssen, R. A. J.; Hummelen, J. C.; Wudl, F. *J. Am. Chem. Soc.* **1995**, *117*, 544. (c) Gonzales, R.; Hummelen, J. C.; Wudl, F. *J. Org. Chem.* **1995**, *60*, 2618. (d) Hall, M. H.; Lu, H.; Shevlin, P. B. *J. Am. Chem. Soc.* **2001**, *123*, 1349. (e) Ouchi, A.; Hatsuda, R.; Awen, B. Z. S.; Sakuragi, M.; Ogura, R.; Ishii, T.; Araki, Y.; Ito, O. *J. Am. Chem. Soc.* **2002**, *124*, 13364.

(4) (a) Haddon, R. C. *Science* **1995**, *378*, 249. (b) Haddon, R. C.; Raghavachari, K. *Tetrahedron* **1996**, *52*, 5207. (c) Weedon, B. R.; Haddon, R. C.; Spielmann, H. P.; Meier, M. S. *J. Am. Chem. Soc.* **1999**, *121*, 335. (d) Williams, R. V. *Chem. Rev.* **2001**, *101*, 1185. (e) Bühl, M.; Hirsch A. *Chem. Rev.* **2001**, *101*, 1153.

(5) (a) Arce, M.-J.; Viado, A. L.; An, Y.-Z.; Khan, S. I.; Rubin, Y. *J. Am. Chem. Soc.* **1996**, *118*, 3775. (b) Rubin, Y. *Chem. Eur. J.* **1997**, *3*, 1012. (c) Qia, W.; Bartberger, M. D.; Pastor, S. J.; Houk, K. N.; Wilkins, C. L.; Rubin, Y. *J. Am. Chem. Soc.* **2000**, *122*, 8333. (d) Qian, W.; Chuang, S.-C.; Amador, R. B.; Jarrosson, T.; Sander, M.; Pieniazek, S.; Khan, S. I.; Rubin Y. *J. Am. Chem. Soc.* **2003**, *125*, 2066.

10.1021/jo0340096 CCC: $25.00
Published on Web 04/04/2003

SCHEME 1. Fulleroid-Methanofullerene Rearrangement.

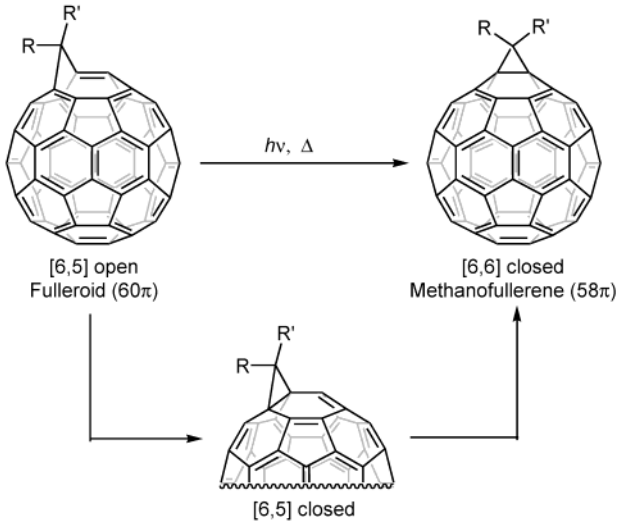

SCHEME 2. Rearrangement Mechanism Proposed by Rubin et al.

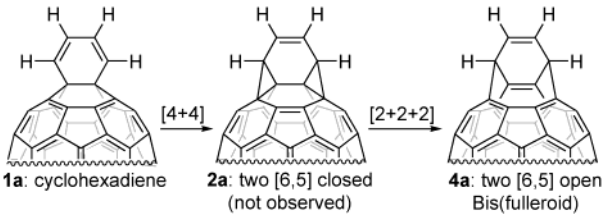

(**2a**), and in the second step the thermally allowed [2+2+2] pericyclic reaction afforded **4a** (Scheme 2). The initial [4+4] photocyclization process has precedent in the classic work of Ginsburg and Masamune on derivatives of 9,10-dihydronaphthalene.[6] Thus, photoisomerization of the cyclohexadiene derivatives has been considered as a general preparation method for bis(fulleroid), and several derivatives synthesized with this method were reported.[7−9] In these papers, neither the formation of other products nor the possibility of other reaction pathways has been mentioned.

Very recently, on the other hand, we found that a photochemical isomerization of the cyclohexadiene derivative **1c** bearing sterically bulky *tert*-butyl esters afforded the desired bis(fulleroid) (**4c**) together with a significant amount of bis(methano)fullerene (**5c**) in which two [6,6] closed units are connected by an ethylene linker (Scheme 3).[9b] In addition, during the reaction, the unexpected formation of a photolabile intermediate **3c** with unsymmetrical [6,5] open/[6,6] closed structure on

SCHEME 3

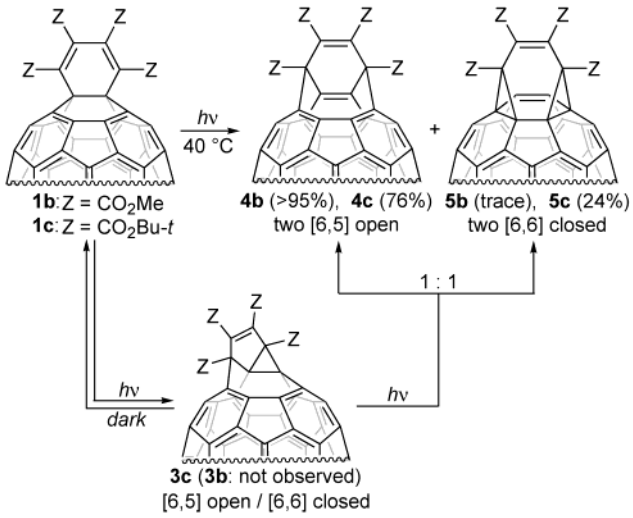

a six-membered ring was recognized. Further we found that the rearrangement of **1b** to **4b** also proceeded thermally.[9c]

These experimental results suggest that there exists another pathway in addition to the [4+4]/[2+2+2] mechanism proposed by Rubin et al.[5a] To clarify the reaction mechanism and the geometrical and electronic features of the products, we carried out theoretical calculations, the results of which will be reported here. Although the size of these large, substituted fullerene derivatives restricts the use of very accurate ab initio and density functional theory techniques, geometry optimizations at the AM1, PM3, RHF, and B3LYP levels were done with Hyper Chem and Gaussian 98.

Calculation Methods

AM1 and PM3 semiempirical methods are the two most popular methods used for the theoretical studies of big molecular systems. Several previous works have showed that the AM1 method is superior to the PM3 method especially for the treatment of fullerene-based systems.[10] In the present work, to arrive at a reasonably good conformation of the heavily substituted reactant and product systems as well as to justify the accuracy of AM1 and PM3 methods, the conformational analysis of smaller systems (basically the substituent units) such as *tert*-butyl formate (**6**), *tert*-butyl acrylate (**7**),[11] di-*tert*-butyl maleate (**8**),[11] and 1,2,3,4-tetra-*tert*-butoxycarbonylcyclohexa-1,3-diene (**9**) is initially carried out with AM1 and PM3 methods (Scheme 4). Several different conformations of **6**, **7**, **8**, and **9** are optimized at these levels of theory. The accuracy of the results is further judged by RHF level optimized geometries of **6**, **7**, and **8**. For the RHF level calculations, the 6-31G* basis set is used. It was found that the most stable geometry optimized at the AM1 level was always in better agreement with the RHF results than the

(6) (a) Babad, E.; Ginsburg, D.; Rubin, M. B. *Tetrahedron Lett.* **1968**, *19*, 2361. (b) Masamune, S.; Seidner, R. T.; Zenda, H.; Wiesel, M.; Nakatsuka, N.; Bigam, G. *J. Am. Chem. Soc.* **1968**, *90*, 5286.

(7) (a) Hsiao, T.-Y.; Santhosh, K. C.; Liou, K. F.; Cheng, C.-H. *J. Am. Chem. Soc.* **1998**, *120*, 12232. (b) Hsiao, T.-Y.; Chidambareswaran, S. K.; Cheng, C.-H. *J. Org. Chem.* **1998**, *63*, 8617.

(8) (a) Murata, Y.; Kato, N.; Komatsu, K. *J. Org. Chem.* **2001**, *66*, 7235. (b) Murata, Y.; Murata, M.; Komatsu, K. *J. Org. Chem.* **2001**, *66*, 8187.

(9) (a) Inoue, H.; Yamaguchi, H.; Suzuki, T.; Akasaka, T.; Murata, S. *Synlett* **2000**, 1178. (b) Iwamatsu, S.; Vijayalakshimi, P. S.; Hamajima, M.; Suresh, C. H.; Koga, N.; Suzuki, T.; Murata, S. *Org. Lett.* **2002**, *4*, 1217. (c) Vijayalakshimi, P. S.; Kitamura, Y. S.; Hamajima, M.; Iwamatsu, S.; Murata, S. Unpublished.

(10) (a) Solà, M.; Duran, M.; Mestres, J. *J. Am. Chem. Soc.* **1996**, *118*, 8920. (b) Mestres, J.; Duran, M.; Solà, M. *J. Phys. Chem.* **1996**, *100*, 7449. (c) Illescas, B. M.; Martín, N.; Seoane, C.; Ortí, E.; Viruela, P. M.; Viruela, R.; de la Hoz, A. *J. Org. Chem.* **1997**, *62*, 7585. (d) Knight, B.; Martín, N.; Ohno, T.; Ortí, E.; Rovira, C.; Veciana, J.; Vidal-Gancedo, J.; Viruela, P.; Viruela, R.; Wudl, F. *J. Am. Chem. Soc.* **1997**, *119*, 9871. (e) Mestres, J.; Solà, M. *J. Org. Chem.* **1998**, *63*, 7556. (f) Manoharan, M.; Proft, F. D.; Geerlings, P. *J. Org. Chem.* **2000**, *65*, 6132. (g) Langa, F.; de la Cruz, P.; de la Hoz, A.; Espíldora, E.; Cossío, F. P.; Lecea, B. *J. Org. Chem.* **2000**, *65*, 2499. (h) Shimotani, H.; Dragoe, N.; Kitazawa K. *J. Phys. Chem. A* **2001**, *105*, 4980.

(11) Akakura, M.; Koga, N. *Bull. Chem. Soc. Jpn.* **2002**, *75*, 1785.

SCHEME 4

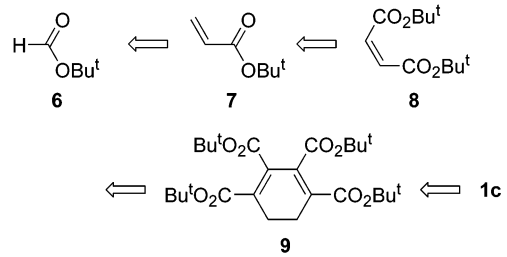

most stable geometry obtained at the PM3 level. Therefore, the AM1 method is chosen as the semiempirical method for the optimization of **9** as well as the heavily substituted fullerene systems. The relevant results of this study on **6**, **7**, **8**, and **9** including the discussion are incorporated in the Supplementary Material.

The different conformations obtained at the AM1 level for **9** are used for the modeling of the butadiene linker of the fullerene system **1c**. The most stable geometry of **1c** is then used for obtaining the geometries of **2c**−**5c** at the AM1 level. These geometries were further optimized by using PM3, RHF/6-31G*, and B3LYP/6-31G* levels. Because of the large size of the molecules, we could not carry out vibrational frequency calculations at the B3LYP/6-31G* level to confirm the nature of stationary points. In the cases of transition states, we performed geometry optimization starting with the structures near the transition state to confirm the connectivity of the transition states. The restricted Slater determinant at the structures of some transition states as well as the intermediates was unstable with respect to becoming the unrestricted determinant. For such structures, we used the unrestricted B3LYP method. Because as shown in the Supporting Information spin contamination is not negligible, we performed spin projection to obtain better energetics. The Hyper Chem 6.0 and GAUSSIAN 98 (Revision A.11) programs were employed for the calculations.[12,13]

Results and Discussion

(a) Tetra-*tert*-butoxycarbonyl-Substituted Cyclohexadiene Derivative of C_{60} (1c). In **1c**, the cyclohexadiene part is similar to the small model compound **9** mentioned in the Calculation Methods section. One major difference is that the saturated C−C linkage is a part of the fullerene system in **1c**. As a result, this C−C linkage that was somewhat flexible in **9** would act as a rigid linkage. This would restrict the conformational space of the substituents of the cyclohexadiene moiety. To obtain the most preferred structure of **1c**, 11 different structures for **1c** were generated from the optimized structures of C_{60} and the 11 conformers of **9** at the AM1 level. Chem3D software was used for this purpose. Using this software, the CH_2−CH_2 linkage of **9** was replaced with the fullerene carbon atoms at the fusion of the two hexagonal rings so that the cyclohexadiene part was somewhat perpendicular to the fullerene surface.

In Figure 1a, the most stable AM1 structure of **1c** is given. In this structure, the C═O groups are positioned in such a way that any two adjacent ones are located above and below the hexadiene C═C−C═C plane. Further, they are twisted inward toward the C═C region. We call this conformation an all-trans conformation. In Figure 1b, the optimized geometry of **1c** at the B3LYP/6-31G* level is also depicted. As we can see, this geometry is very similar to the AM1 geometry. However, in the B3LYP geometry, the substituents at the 2 and 3 positions of the butadiene linker were twisted more toward the butadiene plane as compared to that of the AM1 geometry. In both geometries, the bond length between the two sp^3 carbons of C_{60} (AM1, 1.589 Å; B3LYP, 1.629 Å) was longer than a normal C_{sp^3}−C_{sp^3} single bond, which is in good agreement with the reported values obtained from crystallographic data for the related Diels−Alder adducts of C_{60}.[14] Because of the steric bulkiness of ester substituents, the cyclohexadiene ring is somewhat strained. The torsion angle of the C═C−C═C plane is 6.1° at the B3LYP level (Table 1). Both levels of theory predict that the shortest C═C bond (1.368 and 1.374 Å at AM1 and B3LYP, respectively) on the fullerene cage is the one nearest to the C_{sp^3}−C_{sp^3} bond (Figure 1), showing that the C_{sp^3} atoms break conjugation to enhance bond alternation.

(b) Molecular Structures of 2c, 3c, 4c, and 5c. The all-trans arrangement of the substituents which was most favored in **1c** was assumed in all these structures. At first, AM1 optimized geometries were found for all of them. These geometries were subjected to RHF and followed by B3LYP optimizations. Being more accurate the B3LYP geometries are described in detail (Figure 2 and Table 2).

In the proposed intermediate **2c** (not experimentally observed), the average transannular bond length of the two [6,5] closed cyclopropane rings is 1.629 Å. This long bond distance happens to be the same as the C_{sp^3}−C_{sp^3} bond distance of **1c**. This is similar to the reported value for the [6,5] closed isomer (1.62 Å) and is 0.05−0.07 Å longer than that of the [6,6] closed isomer.[2d] The observed intermediate **3c** has one [6,5] open unit and one [6,6] closed unit. The transannular length of the [6,5] open unit is 2.351 Å, which is slightly longer than that of the fulleroids (calculated structures for C_{60} fulleroids, 2.20−2.25 Å; crystal structure of the C_{70} fulleroid, 2.14 Å).[2d,15] The bridge angle at the sp^3 carbon in the [6,5] open unit is 102.4°. On the other hand, the transannular bond length of the [6,6] closed cyclopropane ring in **3c** is 1.579 Å, which is in good agreement with that of the [6,6] closed isomers (crystal structures of methanofullerene derivatives of C_{60}: 1.57−1.61 Å).[16] As shown in Figure 3, the carbon atom shared by both the [6,5] open and the [6,6] closed units is significantly strained; thus this might be one of the factors in the instability of **3c**.

(12) *HyperChem*; Hypercube, Inc.: 1115 NW 4th Street, Gainesville, FL 32601.

(13) Frisch, M. J.; Trucks, G. W.; Schlegel, H. B.; Scuseria, G. E.; Robb, M. A.; Cheeseman, J. R.; Zakrzewski, V. G.; Montgomery, J. A., Jr.; Stratmann, R. E.; Burant, J. C.; Dapprich, S.; Millam, J. M.; Daniels, A. D.; Kudin, K. N.; Strain, M. C.; Farkas, O.; Tomasi, J.; Barone, V.; Cossi, M.; Cammi, R.; Mennucci, B.; Pomelli, C.; Adamo, C.; Clifford, S.; Ochterski, J.; Petersson, G. A.; Ayala, P. Y.; Cui, Q.; Morokuma, K.; Malick, D. K.; Rabuck, A. D.; Raghavachari, K.; Foresman, J. B.; Cioslowski, J.; Ortiz, J. V.; Stefanov, B. B.; Liu, G.; Liashenko, A.; Piskorz, P.; Komaromi, I.; Gomperts, R.; Martin, R. L.; Fox, D. J.; Keith, T.; Al-Laham, M. A.; Peng, C. Y.; Nanayakkara, A.; Gonzalez, C.; Challacombe, M.; Gill, P. M. W.; Johnson, B.; Chen, W.; Wong, M. W.; Andres, J. L.; Gonzalez, C.; Head-Gordon, M.; Replogle, E. S.; Pople, J. A. *Gaussian 98*, Revision A.11; Gaussian, Inc.: Pittsburgh, PA, 1998.

(14) (a) Rubin, Y.; Khan, S.; Freedberg, D. I.; Yeretzian, C. *J. Am. Chem. Soc.* **1993**, *115*, 344. (b) Khan, S.; Oliver, A. M.; Paddon-Row, M. N.; Rubin, Y. *J. Am. Chem. Soc.* **1993**, *115*, 4919.

(15) Kiely, A. F.; Haddon, R. C.; Meier, M. S.; Selegue, J. P.; Brock, C. P.; Patrick, B. O.; Wang, G.-W.; Chen, Y. *J. Am. Chem. Soc.* **1999**, *121*, 7971.

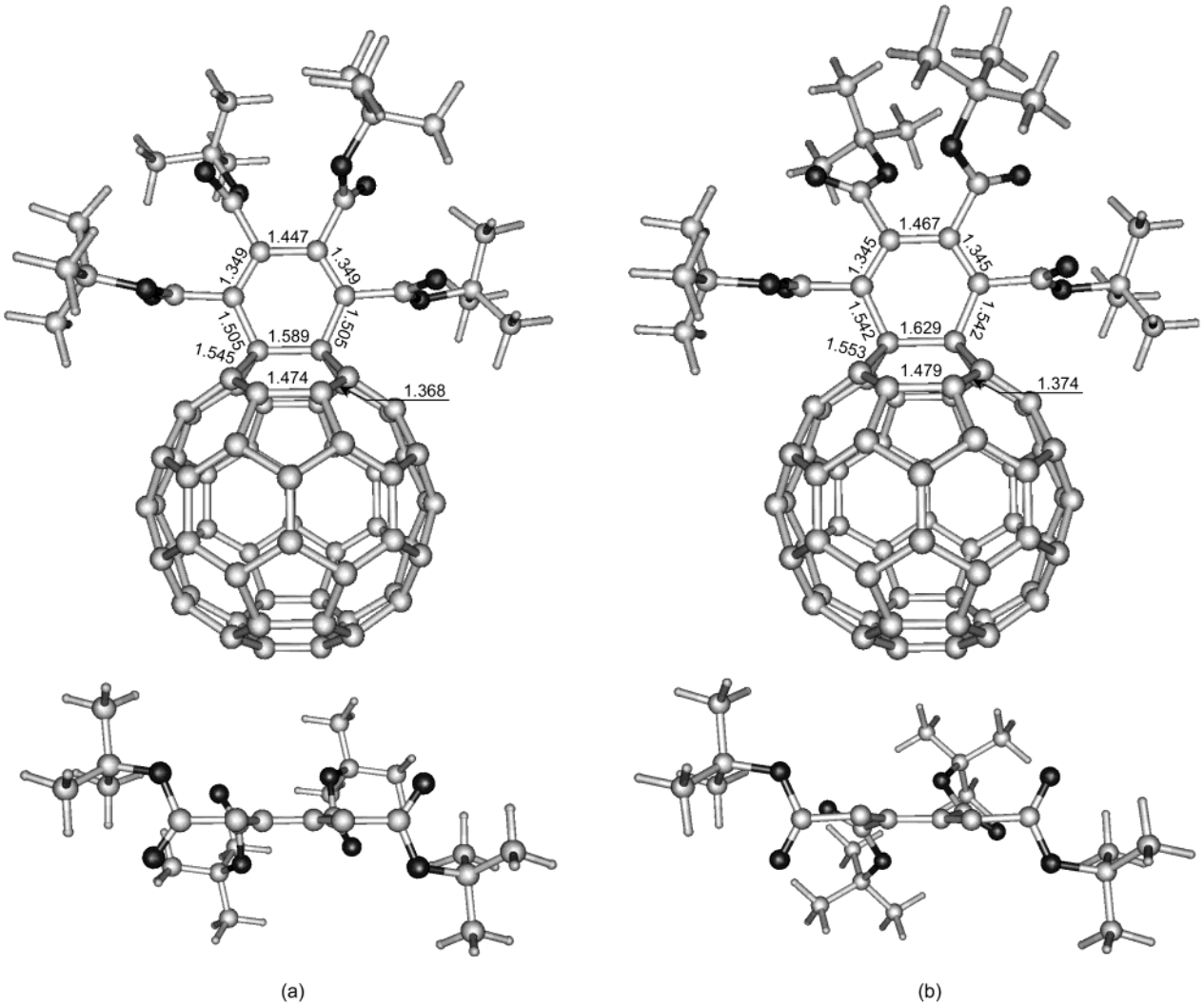

FIGURE 1. (a) AM1 level optimized geometry (in Å) of the most stable conformation of **1c** and (b) the same geometry optimized at the B3LYP/6-31G* level. Partial structures viewed along the C═C−C═C plane are given at the bottom (carbon atoms of C_{60} are omitted for clarity).

TABLE 1. Selected Bond Lengths and Torsion Angles of 1c and 1a (Z = H) at the B3LYP Level

	bond length (Å)			torsion angle (deg)
		ethylene linker		
system	$C_{sp^3}-C_{sp^3}$ on C_{60}	C═C	C−C	ethylene linker C═C−C═C
1c	1.629	1.345[a]	1.467[a]	6.1
1a	1.617	1.337[a]	1.458[a]	0.0

[a] Average of the bond lengths which should be the same due to the molecular symmetry.

In the major product **4c**, the average transannular lengths of the two [6,5] open units is 2.293 Å, which is shorter than the corresponding bond length in **3c**, and the average bridge angle of the sp^3 carbons in [6,5] open units is 97.9°. Meanwhile, in the minor product **5c**, the average transannular bond length of the two [6,6] closed units is 1.582 Å, which coincides with the reported value as well as **3c**. Thus, the DFT approach with the B3LYP method and 6-31G* basis set is a reliable procedure to understand structural features of these systems.

(c) Comparison of the C−C Bonds of the Fullerene Cages of 1c−5c to That of Fullerene. The bond lengths of the [6,6] and [6,5] ring fusions of C_{60} are 1.395 and 1.454 Å, respectively, at the B3LYP/6-31G* level.[17] Compared to C_{60}, in the case of **1c**−**5c**, the shortest [6,6] bonds as well as the longest [6,5] bonds are always found in the $C_{sp^2}-C_{sp^2}$ bonds in the modified six- and five-membered rings (Table 3).

Here the "modified rings" stand for the opened rings or those which have undergone a hybridization change due to addition of the butadiene moiety. For instance, in **1c**, two six-membered and two five-membered rings are modified, and the shortest [6,6] $C_{sp^2}-C_{sp^2}$ bond of 1.374 Å and the longest [6,5] $C_{sp^2}-C_{sp^2}$ bond of 1.479 Å are found in these modified rings (Figure 1b). On the other hand, in the remaining rings there is only a small change

(16) (a) Vogel, E. *Pure Appl. Chem.* **1993**, *65*, 143. (b) Anderson, H. L.; Boudon, C.; Diederich, F.; Gisselbrecht, J.-P.; Gross, M.; Seiler, P. *Angew. Chem., Int. Ed. Engl.* **1994**, *33*, 1628. (c) Osterodt, J.; Nieger, M.; Vögtle, F. J. *J. Chem. Soc., Chem. Commun.* **1994**, 1607. (d) Timmerman, P.; Anderson, H. L.; Faust, R.; Nierengarten, J.-F.; Habicher, T.; Seiler, P.; Diederich, F. *Tetrahedron* **1996**, *52*, 4925.

(17) Choi, C. H.; Kertesz, M.; Mihaly, L. *J. Phys. Chem. A* **2000**, *104*, 102.

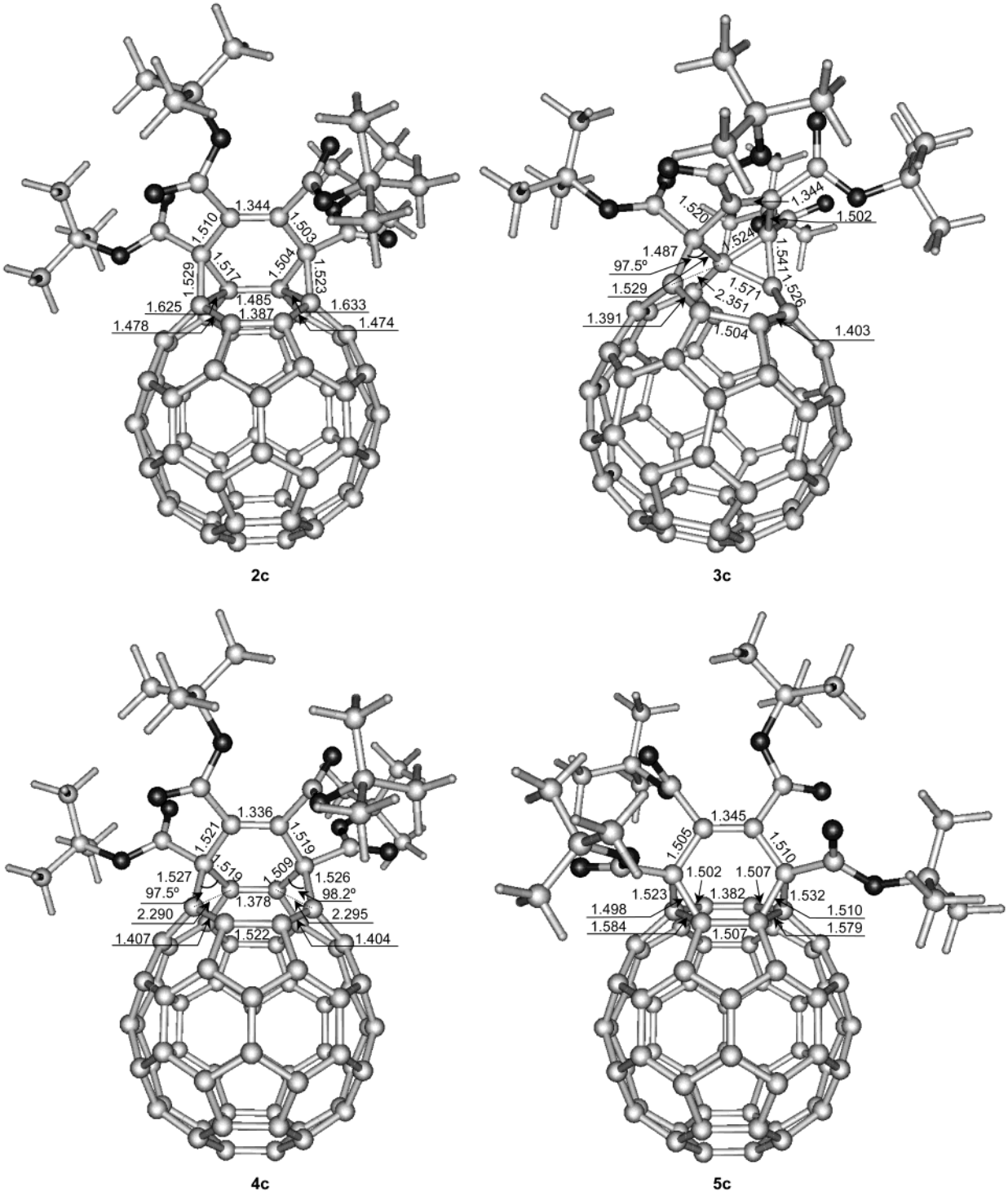

FIGURE 2. B3LYP/6-31G*-optimized molecular structures (in Å) for **2c**−**5c**.

(<0.003 Å) in both the [6,6] and the [6,5] bonds compared to those of fullerene.

(d) Stabilities of Bis(fulleroid) and Bis(methano)-fullerene. The relative energies for compounds **1c**−**5c** at the AM1, PM3, RHF, and B3LYP levels are summarized in Table 4. All these levels of theory agree that the two [6,5] open system **4c** is the most stable structure and that the two [6,5] closed system **2c** is the most unstable structure, in good accordance with experimental results.[9b,18] One significant difference is that, at the AM1 level, **5c** is 14.1 kcal/mol less stable than **1c**, whereas at the B3LYP level it is 3.7 kcal/mol more stable than **1c**. Compound **4c** is 5.7 kcal/mol more stable than **5c** at the B3LYP level. It is important to note that the stability order of bis(fulleroid) and bis(methano)fullerene is completely different from that of fulleroid and methanofullerene[2,3] and is not dependent on substituents.

(e) Calculated NMR Spectra. Structural assignments of compounds **1c**−**5c** were mainly carried out by

(18) The AM1 level method is not sufficient for describing the stability order of fulleroid and methanofullerene. See ref 2d.

TABLE 2. Selected Bond Lengths and Angles for 2c−5c and 3a (Z = H)

	transannular bond length (Å)			bridgehead bridge angle (deg)	ethylene linker bond length (Å)	
system	[6,5] closed	[6,6] closed	[6,5] open	[6,5] open	C=C	C−C
2c	1.629[a]				1.344	1.507[a]
3c		1.571	2.351	102.4	1.344	1.502, 1.520
3a		1.572	2.357	103.1	1.336	1.492, 1.506
4c			2.293[a]	97.9[a]	1.336	1.520[a]
5c		1.582[a]			1.345	1.508[a]

[a] Average bond lengths and angles of the equivalent moieties due to the molecular symmetry.

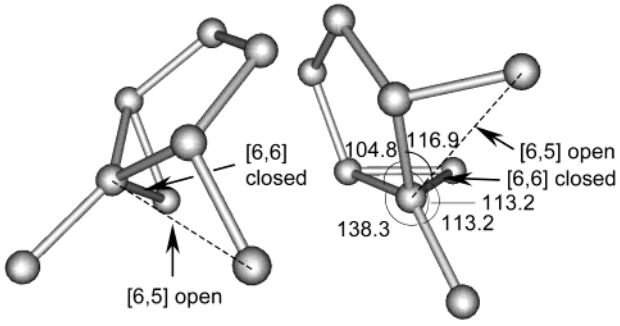

FIGURE 3. Enlarged partial structure of **3c**.

TABLE 3. Bond Lengths of [6,6] and [6,5] Ring Fusions in the Modified Rings of 1c−5c

	[6,6] bond (Å)		[6,5] bond (Å)	
system	longest	shortest	longest	shortest
1c	1.374[a]	1.374[a]	1.479	1.436
2c	1.384	1.379	1.476	1.387
3c	1.403	1.379	1.504	1.428
4c	1.407	1.378	1.522	1.444
5c	1.386	1.382	1.472	1.439

[a] All bond lengths (4 bonds) are equal.

TABLE 4. Relative Energies (in kcal/mol) for 1c−5c[a]

system	AM1	PM3	RHF	B3LYP
1c	0.0 (0.0)[a]	0.0	0.0	0.0 (0.0)[a]
2c	+30.9 (+27.5)[a]	+27.9		+15.9 (+18.9)[a]
3c	+22.3 (+21.0)[a]	+21.9	+12.6	+9.2 (+15.2)[a]
4c	−14.1 (−24.1)[a]	−4.3		−9.4 (−10.8)[a]
5c	+14.1 (+11.2)[a]	+7.8		−3.7 (+0.4)[a]

[a] The relative stability of the corresponding unsubstituted systems **1a**−**5a**.

analyzing the molecular symmetry based on the number of sp^2 signals between 125 and 150 ppm and characteristic sp^3 carbons in the range of 20−85 ppm in the experimental ^{13}C NMR spectra. For **1c**, one sp^3 signal was observed at 64.97 ppm with the C_{2v} symmetric number (17 − 1 + 2 = 18) of sp^2 carbon atoms. C_s symmetric **4c** and **5c** could be distinguished by the number of sp^3 carbons. While one sp^3 signal was observed at 58.55 ppm for **4c**, for **5c** three sp^3 carbon atoms characteristic of the cyclopropane structure were observed at 45.72, 54.08, and 67.63 ppm. In the ^{13}C NMR spectrum of **3c**, four sp^3 signals were observed at 49.53, 57.72, 66.10, and 71.37 ppm with C_1 symmetry. ^{13}C NMR spectra of **3c** and **5c** prepared from 10 to 15% ^{13}C-enriched C_{60} showed that the intensity of the resonance at 49.53 and 71.37 ppm (for **3c**) and at 54.08 and 67.63 ppm (for **5c**) increased significantly in comparison with the other signals (shown by an asterisk in Figure 4).[9b] These results suggest that the chemical shifts of the cyclopropane rings in **3c** and **5c** are quite different, but further characterization of **3c** was rather difficult because of its instability in addition to the unavailability of a comparable compound. Thus we carried out the calculation of magnetic shielding tensors at the B3LYP/6-31G* level using the GIAO method. Shielding constants were converted to chemical shifts by taking the signal of tetramethylsilane as a reference, and the results are summarized in Figure 4.[9b,19] Because the dynamic effect due to the rotations of ester groups is not taken into account in the calculations, the atoms which should be equivalent according to the molecular symmetry have slightly different chemical shifts. As shown in Figure 4, the B3LYP/6-31G* calculation of the ^{13}C NMR chemical shifts for **1c** and **3c**−**5c** can grant an average misfit between the calculated and experimental chemical shifts as low as 7.0 ppm. Therefore, the DFT calculation could be used with confidence to assign all sp^3 carbons.

(f) Mechanism of the Photochemical Rearrangement. It is difficult to explain the formation of the [6,5] open/[6,6] closed structure **3c** and the two [6,6] closed structure **5c** by the previously proposed [4+4]/[2+2+2] mechanism. Is it possible to offer a chemically more intuitive and simple mechanism for this process? The sp^3 carbons in hexadiene **1c** carrying vinyl groups represent the basic structural moiety required for a photochemical di-π-methane rearrangement described in Scheme 5a.[20,21] The primary photoprocess is vinyl−vinyl bridging leading to the formation of the cyclopropyldicarbinyl diradical (**I**), which proceeds to the dihomoallylic 1,3-diradical (**II**), the precursor of the vinylcyclopropane product. According to this equation, the formation of **3c** can be explained as shown in Scheme 5b. First, the C(2)−C(4) bond formation by the di-π-methane rearrangement affords an allylic biradical species bearing one [6,5] closed structure (**10**), which corresponds to **I** in Scheme 5a. Bond cleavage of C(3)−C(4) (formation of **11**, which corresponds to **II** in Scheme 5a) followed by the bond formation of C(2′)−C(3) then affords **3c**.

For **5c**, we confirmed that the photochemical rearrangement of **3c** afforded a 1:1 mixture of **4c** and **5c**.[9b] Because it is well-known for fulleroids that the [6,5] open unit rearranges to the [6,6] closed structure on photoirradiation, formation of **5c** can be explained by the rearrangement of the [6,5] open unit in **3c** to the [6,6] closed cyclopropane ring. On the other hand, the forma-

(19) Calculated chemical shifts for **3c** cited in ref 9b were incorrect. We applied the reported value for TMS (Cheeseman, J. R.; Trucks, G. W.; Keith, T. A.; Frisch, M. J. *J. Chem. Phys.* **1996**, *104*, 5497), but this did not correspond to the fully optimized structure. See: http://www.Gaussian.com/errata.htm.

(20) (a) Zimmerman, H. E.; Grunewald, G. L. *J. Am. Chem. Soc.* **1966**, *88*, 183. (b) Zimmerman, H. E.; Wu, G.-S. *Can. J. Chem.* **1983**, *61*, 866. (c) Zimmerman, H. E.; Armesto, D. *Chem. Rev.* **1996**, *96*, 3065. (d) Zimmerman, H. E.; Církva, V. *J. Org. Chem.* **2001**, *66*, 1839.

(21) (a) Quenemoen, K.; Borden, W. T.; Davidson, E. R.; Feller, D. *J. Am. Chem. Soc.* **1985**, *107*, 5054. (b) Reguero, M.; Bernardi, F.; Jones, H.; Olivucci, M.; Ragazos, I. N.; Robb, M. A. *J. Am. Chem. Soc.* **1993**, *115*, 2073. (c) Wilsey, S. *J. Org. Chem.* **2000**, *65*, 7878. (d) Lewis, F. D.; Zuo, X.; Kalgutkar, R. S.; Wagner-Brennan, J. M.; Miranda, M. A.; Font-Sanchis, E.; Perez-Prieto, J. *J. Am. Chem. Soc.* **2001**, *123*, 11883.

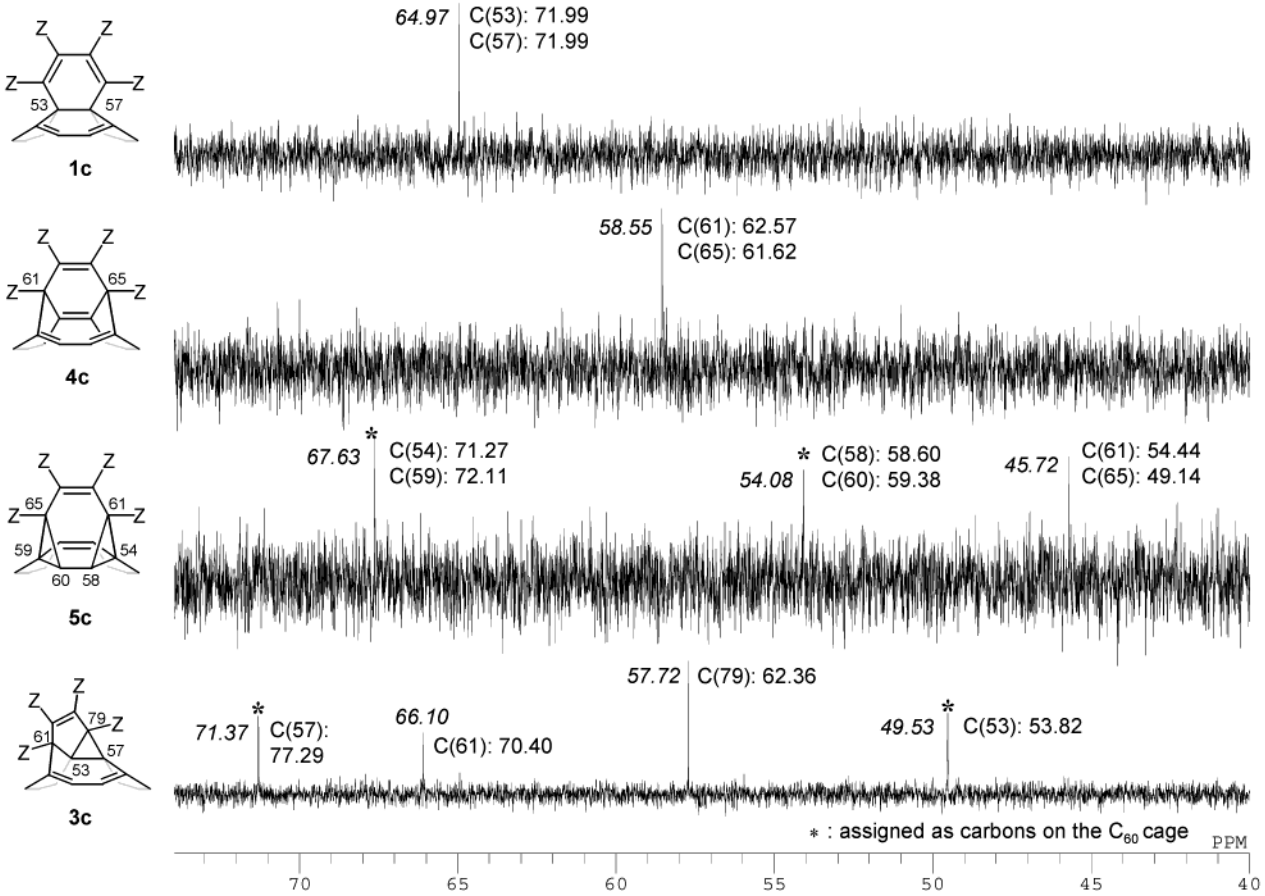

FIGURE 4. Observed and calculated ^{13}C NMR chemical shifts (ppm) for **1c** and **3c**−**5c**. Observed chemical shifts (in C_6D_6) are shown in italics. The signals indicating asterisks are assigned as carbons on the C_{60} cage by using ^{13}C-enriched (10−15%) C_{60} as a starting material. Calculated chemical shifts at the B3LYP/6-31G* level are shown in regular fonts.

tion of **4c** from **3c** is rather difficult to explain. At first, we suspected the formation of **5c** from **4c** by doubly fulleroid−methanofullerene rearrangements, but there is no interconversion between **4c** and **5c** under thermal, photochemical, and acidic conditions.[9b] This means that the photochemical rearrangements of **3c** to **4c** and **3c** to **5c** correspond to two independent mechanisms. We confirmed that the formation of **3c** was reversible and it gradually went back to **1c** in the dark. On the basis of this feature, we suggest that the retrorearrangement might proceed via an intermediate similar to **11**, which may rearrange to **4c** through **12** (vide infra).

As reported before,[9b] the product ratio of **4c**:**5c** was 76:24 in the photochemical rearrangement of **1c**. On the other side, photochemical rearrangement of **3c** gave a 1:1 mixture of **4c** and **5c** under the identical condition. These experimental results suggests that the di-π-methane rearrangement pathway given in this section and the previously proposed [4+4]/[2+2+2] pathway are competitive during the reaction.

(g) Computational Study of the Reaction Mechanism with Model Compounds: Singlet State Calculations. To obtain detailed information on the reaction mechanisms, we performed theoretical calculations on the model reactions. The facts that thermal retrorearrangement from **3c** to **1c** is possible and that the rearrangement of **1b** to **4b** proceeds not only photochemically but also thermally[9c] suggest that there are reaction paths on the singlet potential energy surface. Therefore, we carried out the theoretical calculations for the singlet state rearrangement as well as the triplet state rearrangement. The results for the latter will be discussed in the next section.

Because the size of the systems involved in the reaction prohibits accurate theoretical modeling of the reaction mechanism, we used small model compounds at first. The compound **m-1a** given in Figure 5 is considered the starting material, which represents the model system of unsubstituted **1a**. In this compound, only 28 atoms of the fullerene cage are retained. Moreover, instead of *tert*-butyl ester substituents, hydrogen atoms are used. Starting from **m-1a**, a reaction profile that gives the asymmetric product (**m-3a**) and the two [6,5] open product (**m-4a**) is calculated at the unrestricted AM1 (UAM1) level. Here, **m-3a** and **m-4a** can be considered as model systems for **3a** and **4a**, respectively. In the calculation, the singlet states of the systems are always used. As shown in Figure 5, **TS1** and **TS2** correspond to the TSs for the formation of the intermediates one [6,5] closed (**13**) and one [6,5] open (**14**) structures, respectively. The intermediate **14** can go to either **m-3a** or **m-4a** via **TS4** and **TS3**, respectively. At the UAM1 level, the transformation of **m-1a** to both **m-3a** and **m-4a** takes place in 3 steps with the highest activation energy of 33.7 kcal/mol required for the first [6,5] ring closing step. However, single-point energy calculations at the UB3LYP/6-31G*

SCHEME 5. (a) Di-π-methane Rearrangement[a] and (b) Possible Rearrangement Pathway[b]

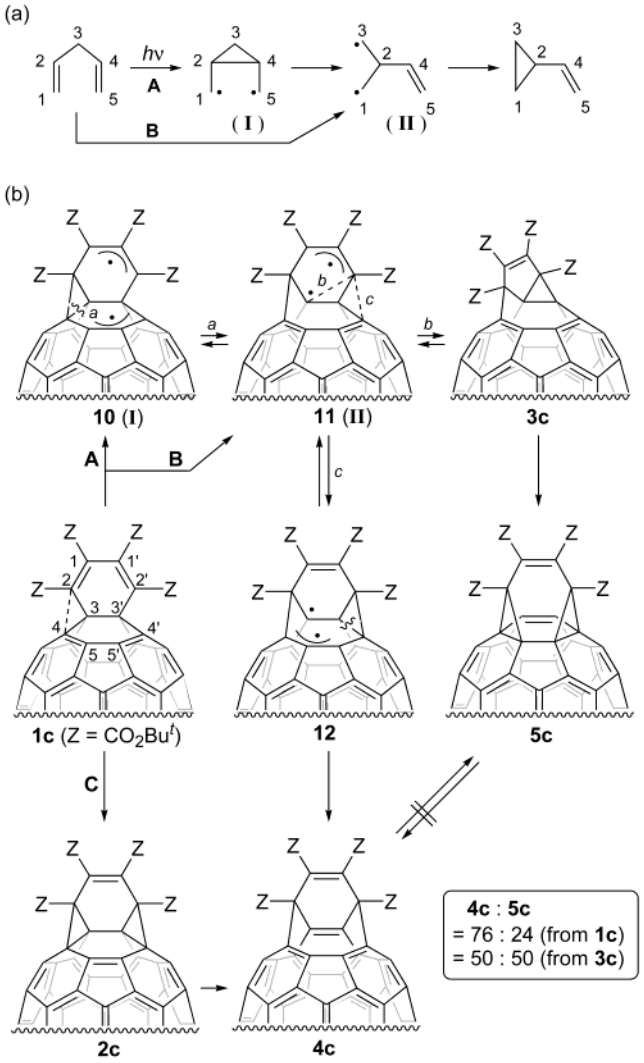

[a] **A**: Zimmerman mechanism. **B**: Bernardi, Rob mechanism.[20c] [b]**A**, **B**: Di-π-methane rearrangement mechanism. **C**: [4+4]/[2+2+2] mechanism proposed by Rubin.[5a]

level for the UAM1 structures show that the relative stabilities of these systems gradually decrease in the following order: **m-1a**, **TS1**, **13**, **TS2**, **14**, **TS3**. This suggests that elementary reactions are combined to result in only one TS; for the path leading to **m-4a** it is similar to **TS3** and for **m-3a** it is **14** or **TS2**.

To clarify this feature with more reliable calculations, we determined the structures of the stationary points for the reaction of **1a** at the UB3LYP/6-31G* level. Compared to the **m-1a** model system, all the carbon atoms of the fullerene cage are considered for **1a**. In the calculations, only one **TS5** is located as shown in Figure 6. The structural features of this TS are somewhat similar to those of **TS2**. Attempts to find TSs connecting **1a** and **4a** failed and they finally converged to **TS5**. These results show that the **1a** to **3a** conversion in the singlet state takes place in one step through **TS5** with an activation energy of 41.8 kcal/mol and that there is no reaction path directly connecting **1a** and **4a**. **TS3** for the smaller model system is the least stable among the stationary points at the UB3LYP level, suggesting that the reaction valley connecting **1a** and **4a** on the potential energy surface does not exist at the UB3LYP level. The structure of **TS5** shows that during the reaction of **3a** to **1a**, first the C−C bond of the [6,6] cyclopropane ring which consists of the five-membered ring (1.522 Å in **3a**) is almost broken (2.457 Å in **TS5**), the C−C bond of the [6,5] ring fusion is partially formed (1.952 Å), and the C−C bond in the [6,5] open structure (1.528 Å) is then broken at a very late stage of the reaction. These structural features are consistent with those found on the UAM1 potential energy surface. The energy barrier from **3a** to **1a** is 26.6 kcal/mol, which is 15.2 kcal/mol smaller than that from **1a** to **3a**. This points out that the retrorearrangement from **3c** to **1c** is a more favorable thermal process than the rearrangement of **1c** to **3c**.

(h) Computational Study of the Reaction Mechanism with Model Compounds: Triplet State Calculations. The photochemical rearrangement of **1c** to **4c** and **5c** is concluded to proceed competitively through both the [4+4]/[2+2+2] and the di-π-methane rearrangement mechanisms. Concerning the latter, the photochemical rearrangement of fulleroids to methanofullerenes has also been explained by the di-π-methane rearrangement,[3b] and Wudl et al. pointed out that, in the case of fullerene derivatives, the rearrangement proceeds via the triplet manifold because (i) rigid (bycyclic)-molecules are known to react via the triplet state[20b] and (ii) the intersystem crossing in C_{60} is very efficient.[1] In fact, the photochemical rearrangement of **1c**, as well as the fulleroid−methanofullerene rearrangement, was extremely retarded in atmospheric air.[3b,d,9c] Therefore, we consider the triplet state of **1c** and the possible reactions starting from it on the triplet state potential energy surface for understanding the photochemical rearrangements, especially for estimation of the two possible pathways of the biradical structure **11** (paths *b* and *c* in Scheme 5b). Because of the size of the systems, hydrogen atoms are used instead of *tert*-butyl ester substituents. The unrestricted B3LYP/6-31G* level of theory is used for the calculations.

In Figure 7, the triplet state potential energy profile (solid lines) is depicted. At first, the excited state **1a** in the triple state passes through transition state **TS6** for the first [6,5] ring closing and one [6,5] closed structure **15** forms. The activation energy for this step is 8.1 kcal/mol. In the next step, the cyclopropane ring of **15** opens up at the [6,5] ring fusion with an activation energy of 5.5 kcal/mol. The TS corresponding to this step is **TS7**, and the product is the one [6,5] open structure **16**, which corresponds to **11** in Scheme 5b. It is found that **16** can give **4a** and **3a** if it passes through the transition states **TS8** and **TS9**, respectively. The formation of the former (**4a**) is more preferred because of the small activation energy of 7.8 kcal/mol required for it compared to the high activation energy of 26.6 kcal/mol needed for the formation of the latter (**3a**). However, both activation energies are slightly high, especially for the latter.

Figure 7 also depicts the relative spin-projected singlet state energies corresponding to all the triplet state geometries (broken lines).[22] A comparison of this spin-projected singlet state potential energy profile with the triplet state potential energy profile leads to some interesting conclusions. The singlet states of **1a** and **TS6**

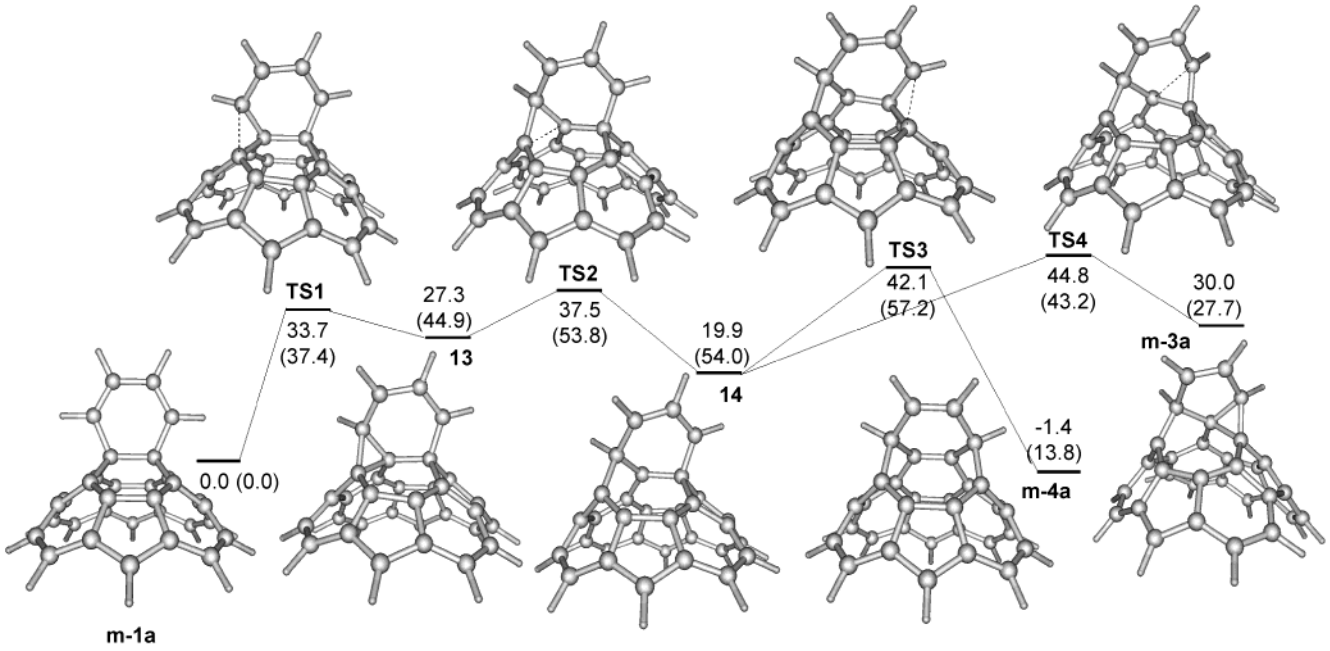

FIGURE 5. Singlet state reaction profile for the model compound at the UAM1 level. Relative energies at the UAM1 level are shown in regular font. Relative energies for the UB3LYP/6-31G* single-point energy calculation with use of UAM1 geometries are also shown in parentheses.

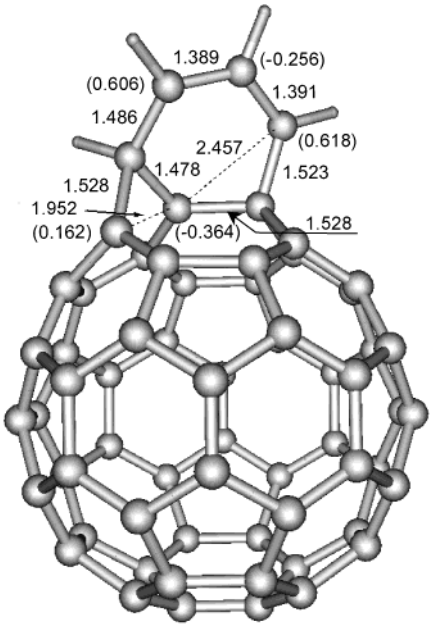

FIGURE 6. Structure of **TS5** (in Å) and relative energies at the UB3LYP/6-31G* level. Spin populations higher than ±0.15 are shown in parentheses.

are more stable than the corresponding triplet states. However, the intermediates **15** and **16**, and **TS7** are more stable on the triplet state potential energy surface. On the other hand, the reaction paths from **16** to **4a** and **16** to **3a** are more favored on the singlet state potential energy surface. This strongly suggests the possibility of the occurrence of the intersystem crossing in which **16** transforms toward **TS8** or **TS9**. If that happens, the formation of **3a** from **16** is almost free of barriers, and for the formation of **4a**, approximately 4.4 kcal/mol of energy is needed. These results suggest that rearrangement proceeded initially through the triplet state to give **16** followed by the intersystem crossing to give **3a** and **4a**. On the basis of the results and discussion in this section and the previous section, a reaction scheme that will fit the experimental and theoretical studies is proposed in Scheme 6.

(i) Difference between the Fulleroids and Bis(fulleroid)s. Among the C_1 derivatives of fullerenes, methanofullerene derivatives are generally more stable than those of fulleroids. On the other hand, as shown in the previous section, bis(fulleroid) is more stable than the bis(methano)fullerene. It can be noted that three main factors, viz., (1) retention of the 60π electron spherical conjugation, (2) the presence of homoaromaticity, and (3) the release of the ring strain due to the opening of two pentagons, account for the higher stability of bis(fulleroid). However, among these three factors, the contribution from the first two factors may be the same for mono(fulleroid) and bis(fulleroid). In the case of fulleroid, the homoaromaticity, as well as homoconjugation, is quite appreciable as concluded by Haddon et al.[4b] In the case of bis(fulleroid), the homoconjugation can exist at two transannular bonds compared to one in fulleroid. However, the transannular bonds in bis(fulleroid) are slightly longer than that of a typical fulleroid, indicating a weaker homoconjugation in the former as compared to the later. Therefore, the most important factor that accounts for the stability of the bis(fulleroid) might be the opening of the two pentagons. In this process, the release of ring strain in the C_{60} cage may be much higher than that achieved in the opening of one pentagon in the case of fulleroid. For instance, the

(22) (a) Yamaguchi, K.; Jensen, F.; Dorigo, A.; Houk, K. N. *Chem. Phys. Lett.* **1988**, *149*, 537. (b) Yamanaka, S.; Kawakami, T.; Nagao, H.; Yamaguchi, K. *Chem. Phys. Lett.* **1994**, *231*, 25. (c) Goldstein, E.; Beno, B.; Houk, K. N. *J. Am. Chem. Soc.* **1996**, *118*, 6036.

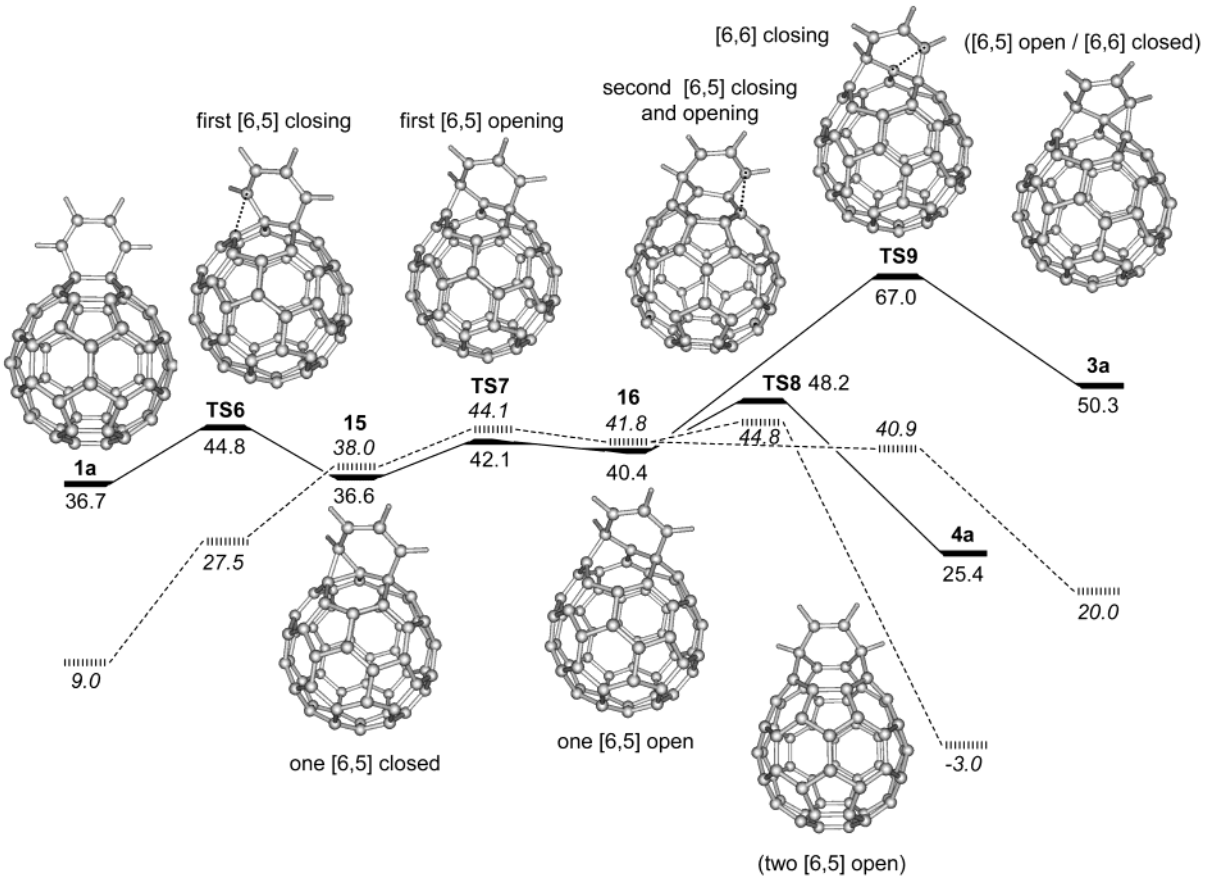

FIGURE 7. Triplet state potential energy profile (solid lines) and the corresponding projected singlet state potential energy profile (broken lines) obtained from the triplet state geometries. The relative energies (in kcal/mol) are also depicted. The 0.0 point is taken as the singlet state of **1a**.

SCHEME 6

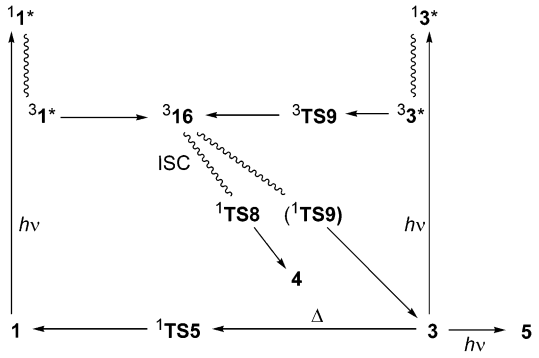

elongation of the transannular bond lengths by ∼0.1 Å and the widening of the bond angle at the bridge head position by ∼5.0° in bis(fulleroid) compared to the fulleroid support this fact.

Conclusions

In the present paper, it has been shown that the DFT approach using the B3LYP with the 6-31G* basis set is a particularly reliable procedure to understand the structure and properties of these systems. At all levels of theory, bis(fulleroid) was found to be more stable than the corresponding bis(methano)fullerene. This is in sharp contrast to the fulleroid−methanofullerene relationship. The stability of bis(fulleroid) is mainly derived from its two [6,5] open structure that releases a substantial amount of strain energy of the fullerene cage. A labile intermediate with the [6,5] closed/[6,6] closed structure was more stable than the previously proposed two [6,5] closed intermediate structure, and the formation of this compound is well explained by using the di-π-methane rearrangement. The two pathways, the symmetrical [4+4]/[2+2+2] and the unsymmetrical di-π-methane route, described in this paper are competitive during the reaction.

Acknowledgment. This research was partly supported by Grant in Aids for Scientific Research No. 14044036 and 14350475 from the Minister of Education, Culture, Sports, Science and Technology, Japan. Part of calculations were carried out at the Center of the Institute for Molecular Science. We thank Prof. T. Suzuki (Institute for Molecular Science, Japan) for valuable discussions and Ms. Y. Mineo and Mr. Y. Andoh (Nagoya University) for technical support.

Supporting Information Available: Conformational studies of substituent units (**6**, **7**, **8**, and **9**) and Cartesian coordinates optimized by using the B3LYP/6-31G* method. This material is available free of charge via the Internet at http://pubs.acs.org.

JO0340096